ISRIB prevents synaptic plasticity disruption and cognitive deficits in live rat model of Alzheimer's disease

Neng-Wei Hu (hunw@tcd.ie)
Trinity College Dublin: The University of Dublin Trinity College https://orcid.org/0000-0001-5571-296X
Zhengtao Hu
Zhengzhou University
Pengpeng Yu
Zhengzhou University
Deguo Wang
Wannan Medical College
Yong Wu
Wannan Medical College
Yingjie Qi
Trinity College Dublin: The University of Dublin Trinity College
Tomas Ondrejcak
Trinity College Dublin: The University of Dublin Trinity College
Igor Klyubin
Trinity College Dublin: The University of Dublin Trinity College
Jitian Xu
Zhengzhou University
Yin Yang
Zhengzhou University
Michael J. Rowan
Trinity College Dublin: The University of Dublin Trinity College

Research article

Keywords: Alzheimer's disease, amyloid-β protein, integrated stress response, endoplasmic reticulum stress, ISRIB, long-term depression, cognitive deficit

Posted Date: October 12th, 2020

DOI: https://doi.org/10.21203/rs.3.rs-88220/v1

Abstract

Background

Growing evidence shows that targeting the integrated stress response (ISR) through the inhibition of phosphorylation of eIF2α provides beneficial effects in animal models of neurodegenerative diseases including Alzheimer's disease (AD). However, those results are inconsistent and somehow conflicting likely due to the important role of ISR in both cell death and survival. Aβ-triggered pathologies including microvascular hypoxia, neuronal hyperactivation, neuroinflammation are common inducers of the ISR. The small-molecule inhibitor of the ISR called ISRIB, which only partially restores protein synthesis and confers neuroprotection without adverse effects on the pancreas most probably due to its state-dependent action, remarkably enhances cognition in animals.

Methods

To elucidate the roles of ISR in AD pathogenesis, we systemically treated exogenous Aβ-injected animals with ISRIB. Both Aβ-facilitated long-term depression (LTD) and Morris water maze were used to characterize Aβ-induced dysfunction.

Results

Acute treatment with ISRIB prevented Aβ-facilitated LTD and repeated treatment abrogated the spatial learning and memory deficits in exogenous Aβ-injected animals. Moreover, ISRIB restored aberrant high level of ATF4 to normal but did not affect the aberrant high level of phosphorylated eIF2α in the hippocampus of exogenous Aβ-injected rats.

Conclusions

Targeting the ISR by suppressing the eIF2α cascade with ISRIB may provide protective effects against the synaptic and cognitive disruptive effects of Aβ which likely mediate the early stage of sporadic AD.

Background

The major adaptive gene expression program to cellular stress termed the "integrated stress response" (ISR) is induced by external factors including essential nutrient deprivation and viral infection. Similarly, intrinsic cell stress such as endoplasmic reticulum (ER) stress (e.g. that caused by the accumulation of unfolded proteins, or potentially damaging changes in cellular homeostasis) triggers a range of protective actions, including the ISR as part of the unfolded protein response (UPR). Central to the ISR is the regulation of translation initiation via phosphorylation of the eukaryotic initiation factor 2 α-subunit (eIF2α) to preserve protein homeostasis. eIF2α phosphorylation by PKR-like ER kinase (PERK), a component of the UPR, and three other eIF2α kinases (GCN2, PKR and HRI), is a highly conserved mechanism regulating translation initiation (1, 2).

As part of the acute adaptive response, general protein synthesis is suppressed temporarily, which promotes proteostasis but also inhibits protein synthesis-dependent synaptic plasticity and memory mechanisms (1). At the same time, the synthesis of activating transcription factor 4 (ATF4) is increased, which amongst other things, promotes negative feedback control of eIF2α phosphorylation. With very strong or prolonged stress the ISR becomes maladaptive and apoptosis can be triggered via ATF4 (3, 4). In the brains of patients with Alzheimer's disease (AD) elements of the UPR and ISR are persistently dysregulated, with PERK upregulation and translational dysregulation due to aberrant eIF2α phosphorylation being well documented(5–7). Importantly, inhibition or genetic reduction of PERK or other eIF2α kinases (GCN2, PKR and HRI) is protective in many different animal models of neurodegeneration including some models of AD (8–10).

Of particular potential therapeutic value, a brain-penetrant small molecule ISR inhibitor, called ISRIB, which restores translation downstream of kinase phosphorylation of eIF2α, by activating the nucleotide exchange factor eIF2B (11–13), has been found to have beneficial effects in neurodegeneration models (14), but without the pancreatic toxicity of PERK inhibitors, presumably because its action is state-dependent (15).

To determine whether ISRIB may be beneficial in early sporadic AD, we chose to study the disruptive effects of injecting exogenous amyloid-β-protein (Aβ) (both soluble Aβ-containing AD brain extract and synthetic $A\beta_{1-42}$) in rats. We found that pre-treatment with ISRIB completely prevented AD brain extract-facilitated LTD and abrogated a learning and memory deficit caused by synthetic $A\beta_{1-42}$ in the Morris water maze (MWM). Moreover, we observed that pre-treatment with ISRIB restored aberrant high level of AFT4 without affecting p-eIF2α in the hippocampus of exogenous Aβ-injected rats. Suppressing eIF2α cascade may underlie the beneficial effects of ISRIB on Aβ-mediated synaptic plasticity disruption and spatial learning and memory deficits.

Methods

Animals

Animal care and experimental protocols followed the ARRIVE (Animal Research: Reporting of In Vivo Experiments) guidelines 2.0 (16) and were approved by the Health Products Regulatory Authority, Ireland and Animal Care and Use Committee of Zhengzhou University and Wannan Medical College, China. All efforts were made to minimize the number of animals used and their suffering.

Adult (250-350g, 8-11 weeks old) male Wistar and Lister Hooded rats were provided by the Comparative Medicine Unit of Trinity College Dublin and the Laboratory Animal Center of Zhengzhou University and Nanjing University. The animals were housed under a 12h light-dark cycle at room temperature (19-22^{o}C). Prior to the acute experiments, animals were anesthetized with urethane (1.5-1.6 g/kg, i.p.). Lignocaine (10 mg, 1% adrenaline, s.c.) was injected over the area of the skull where electrodes and screws were to be implanted. The body temperature of the rats was maintained at 37-38 ^{o}C with a feedback-controlled

heating blanket. For i.c.v. injection of synthetic Aβ, the animals were anaesthetized with ketamine (80 mg/kg, i.p.) and xylazine (8 mg/kg, i.p.). The animals were monitored until full consciousness was regained and housed singly for one week or until wound healing had completed, after which they were housed in pairs with continuous access to food and water *ad libitum.*

Electrophysiology

Electrodes were made and implanted as described previously (17). Briefly, monopolar recording electrodes were constructed from Teflon-coated tungsten wires (75 μm inner core diameter, 112 μm external diameter) and twisted bipolar stimulating electrodes were constructed from Teflon-coated tungsten wires (50 μm inner core diameter, 75 μm external diameter) separately. Field excitatory postsynaptic potentials (EPSPs) were recorded from the stratum radiatum in the CA1 area of the right hippocampus in response to stimulation of the ipsilateral Schaffer collateral-commissural pathway. Electrode implantation sites were identified using stereotaxic coordinates relative to bregma, with the recording site located 3.4 mm posterior to bregma and 2.5 mm lateral to midline, and stimulating site 4.2 mm posterior to bregma and 3.8 mm lateral to midline. In some animals, another stimulating electrode was implanted at a site located 2.5 mm posterior to bregma and 2.2 mm lateral to the midline. The final placement of electrodes was optimized by using electrophysiological criteria and confirmed via postmortem analysis.

Test EPSPs were evoked by a single square wave pulse (0.2 ms duration) at a frequency of 0.033 Hz and an intensity that triggered a 50% maximum EPSP response. LTD was induced using 1 Hz low frequency stimulation (LFS) consisting of 900 pulses (0.2 ms duration). During the LFS the intensity was raised to trigger EPSPs of 95% maximum amplitude. A relatively weak LFS protocol, used to study the Aβ-mediated facilitation of LTD, consisted of 300 pulses (0.2 ms duration) at 1 Hz, with an intensity that evoked 95% maximum amplitude. None of the conditioning stimulation protocols elicited any detectible abnormal changes in background EEG, which was recorded from the hippocampus throughout the experiments.

A stainless-steel cannula (22 gauge, 0.7 mm outer diameter) was implanted above the right lateral ventricle (1 mm lateral to the midline and 4 mm below the surface of the dura). The solutions were injected in a 5 μL volume over a 3-min period or 10 μL volume over a 6-min period via an internal cannula (28 gauge, 0.36 mm outer diameter). Verification of the placement of cannula was performed postmortem by checking the spread of ink dye after i.c.v. injection.

Morris water maze

Two weeks after a single i.c.v. injection of soluble $A\beta_{1-42}$ or reverse control $A\beta_{42-1}$ under recovery anaesthesia, the rats were trained in a water pool (150 cm diameter) with a hidden platform of 10 cm diameter. Animals were handled daily for 3 days before the experiment, and the training protocol consisted of four swimming trials per day. A relatively weak protocol consisted of one swimming trial per day. Each animal swam until it found the hidden platform or 120 s, when it was gently guided to the platform and stayed there for 10 s before being returned to the cage. Immediately after the swimming

trial the animals were injected intraperitoneally with ISRIB (0.25 mg/kg in saline, 1% DMSO). For the probe test, the platform was removed and each animal was allowed to swim for 120 s, while its swimming trajectory was monitored with a video tracking system (Smart, PANLAB, Spain).

Western blot

Animals were sacrificed with decapitation after finishing experiments. The whole brain was taken out and the hippocampus were separated from other parts and then all the brain tissues were immediately frozen in liquid nitrogen and stored at -80^{o}C. The rat hippocampus was homogenized Tris-HCl buffer (10mM Tris-HCl, pH 7.5, 150mM NaCl, and 0.5% Triton X-100, 0.1mM PMSF) containing 1% protease inhibitor mixture and 1% phosphatase inhibitor mixture (Sigma-Aldrich,). Protein concentration was determined by the Bradford technique (Bio-Rad Laboratories), and equal amounts of protein from each sample were loaded on 10% Tris-glycine SDS-PAGE (Invitrogen) gels. The protein were transferred onto PVDF membranes (Millipore, IPVH00010), After transfer, membranes were blocked for at least 60 min at room temperature with blocking buffer (BB; 5% non-fat milk in TBS containing 0.1% Tween 20 (TBS-T)), then probed overnight at 4 °C using the following primary antibodies, rabbit anti-phospho-eIF2α (Ser51) (1: 500, ab32157, Abcam), rabbit anti-total eIF2α (1: 1000, A0764, ABclonal), rabbit anti-ATF4 (1: 1000, ab23760, Abcam) and rabbit anti-GAPDH (1: 1000, AC001, ABclonal), washed three times use TBST then incubated with the secondary antibody goat anti-rabbit (1:10,000, 111-035-144, Jackson ImmunoResearch) for 2h at room temp. And the proteins were visualized by the chemiluminescence reagents provided with the ECL kit (Affinity Biosciences) and then detected with a machine of ProteinSimple (FluorChem E, USA). And then used the ImageJ to quantify the intensities of the blot.

TBS Extract of Human Brain

The same human brain tissue was used as our previous report (17). Human brain tissue was used in accordance with local Ethics Committee guidelines. Briefly, tris-buffered saline (TBS) extracts of brain specimens were prepared, processed and analyzed as described previously. Frozen cortex (0.9 g) was allowed to thaw on ice, chopped into small pieces and homogenized in 4.5 ml of ice-cold 20 mM Tris-HCl, pH 7.4, containing 150 mM NaCl with 25 strokes of a Dounce homogenizer (Fisher, Ottawa, Ontario, Canada). Water-soluble Aβ was separated from membrane-bound and plaque Aβ by centrifugation at 91,000g and 4^{o}C in a TLA 55 rotor (Beckman Coulter, Fullerton, CA, USA) for 78 minutes. To eliminate bioactive small molecules the supernatant was exchanged into ammonium acetate. Thereafter, extracts were divided into 2 parts: one aliquot was immunodepleted of Aβ by 3 rounds of 12-h incubations with the anti-Aβ antibody, AW8, and protein A at 4^{o}C. The second portion was not manipulated in any way and is simply referred to as AD. Aliquots of samples were stored at -80^{o}C .

Synthetic Aβ

Soluble A$\beta_{1\text{-}42}$ and reverse control A$ß_{42\text{-}1}$ (ChinaPeptides, Shanghai) was prepared as a stock solution of 75 μM in mild alkali (0.1% ammonium hydroxide) in milliQ water to avoid isoelectric precipitation, and

then centrifuged at 100,000 x g for 3 h to remove any fibril aggregates. An aliquot of the supernatant was taken to estimate peptide concentration using the micro BCA protein assay (Thermo-Fisher Scientific Life Science Research Products, Rockford, IL) and the remaining supernatant was stored at -80 ^{o}C until required.

Pharmacological agents

Emetine dihydrochloride hydrate (Emetine, Sigma, E2357) was prepared in ultra-clean water. **Trans-N,N'-(Cyclohexane-1,4-diyl)bis(2-(4-chlorophenoxy) acetamide** (ISRIB, Sigma, **SML0843**) was dissolved in DMSO with gentle warming and diluted in polyethylene glycol 400 (PEG400) or saline before injection; 1:1 DMSO and PEG400 or 1 % v/v solution of DMSO in saline was used as vehicle control.

Data analysis.

Values are expressed as the mean ± s.e.m. For the electrophysiology experiments, the last 10 min prior to LFS was used to calculate the "Pre" –induction fEPSP amplitude. Unless otherwise stated the magnitude of LTD was measured over the last 10 min at 3 h after ("Post") LFS. Control experiments were interleaved randomly throughout. To compare between two group with one time point, unpaired *t* test was used. To compare between groups of three or more, one-way ANOVA with Bonferroni multiple comparisons was used. A two-tailed paired Student's *t*-test (paired *t*) was used to compare between "Pre" and "Post" within groups. For the Morris water maze test, two-way ANOVA followed by a *post hoc* Bonferroni multiple comparisons test was used for escape latency analysis and one-way ANOVA with Bonferroni multiple comparisons was used to analyze the results from the probe trials. For the Western blots, one-way ANOVA with Bonferroni multiple comparisons was used. A value of $P < 0.05$ was considered statistically significant.

Results

ISRIB restores protein synthesis dependence of Aβ-facilitated LTD at CA3-to-CA1 synapses *in vivo*

Protein synthesis provides a mechanism for the persistence of memory and is important in the late phase of many forms of synaptic plasticity including LTD (18) (but see (19)). Previously we reported that Aβ usurps normal mechanisms of LTD at glutamatergic synapses between CA3 and CA1 hippocampal pyramidal neurons in the acutely anaesthetized adult rat (17) but the role of protein synthesis in this form of LTD is still unclear. To investigate this, we tested the ability of the protein synthesis inhibitor emetine and ISRIB, an agent which restores protein synthesis, to modulate control LTD and Aß-facilitated LTD in anaesthetized rats.

Synaptic transmission was measured in the stratum radiatum of CA1 area of the dorsal hippocampus following stimulation delivered to the Schaffer collateral-commissural pathway. The application of strong LFS, consisting of 900 high intensity pulses at 1 Hz (LFS-900), triggered synaptic LTD that was stable for more than 3 h **(Fig. 1ab)**. The application of a peri-threshold relatively weak LFS of 300 high intensity

pulses at 1Hz (LFS-300) did not induce persistent depression in vehicle-injected rats but induced robust and stable LTD in rats with acute intracerebroventricular (i.c.v.) injection of water soluble SDS-stable Aβ in post-mortem AD brain extracts (AD-Aβ) **(Fig. 1cd)**.

Because previous reports indicate that the protein synthesis dependence of LTD is disrupted under certain pathological conditions(19) , we postulated that Aβ-facilitated-LTD would be resistant to protein synthesis inhibitors. Consistent with this prediction, the protein synthesis inhibitor emetine, at a dose (434 nmol, i.c.v.) that completely blocked our control LTD induced by LFS-900 **(Fig. 1ab),** did not affect the LTD induced by LFS-300 in the presence of soluble AD-Aβ **(Fig. 1cd)**. Intriguingly systemic administration of ISRIB (3mg/kg), which can partially restore protein synthesis (14), blocked AD-Aβ facilitated LTD induced by LFS-300 **(Fig. 2cd)** while it did not affect control LTD induced by LFS-900 **(Fig. 2ab)**.

Our previous studies indicate that the neurotoxicity of water soluble SDS-stable Aβ in post-mortem brain extracts is mimicked by oligomeric $A\beta_{1\text{-}42}$ (17). Therefore, we continued to investigate the effect of ISRIB on animals treated with soluble oligomeric $A\beta_{1\text{-}42}$ via i.c.v. injection.

ISRIB abrogates spatial memory deficits in exogenous Aβ-injected rats

Recent growing evidence suggests that synaptic LTD is a bona fide hippocampal learning and memory mechanism (20-22) and soluble Aβ-facilitated LTD may underlie learning and memory deficits in early AD (23, 24). I.c.v. or intrahippocampal injection of exogenous soluble Aβ can cause spatial learning and memory deficits in rats and mice (25-27). Having found that systemic administration of ISRIB successfully prevented AD brain Aβ-facilitated LTD in anaesthetized rats, we next determined whether systemic administration of ISRIB impacted spatial learning deficits in rats injected with soluble synthetic Aβ in the Morris water maze.

Water maze training with standard protocols (4 trials per day) was started 2 weeks after i.c.v. injection of $Aß_{1\text{-}42}$ or reverse control $Aß_{42\text{-}1}$. ISRIB (0.25 mg/kg, i.p.) or vehicle was injected immediately after the last training trial every day. Whereas repeated training caused a day-to-day decrease in escape latency in the sham surgery group or $A\beta_{42\text{-}1}$ injected group (rats that had been injected i.c.v. with the reverse sequence peptide $A\beta_{42\text{-}1}$), $A\beta_{1\text{-}42}$ inhibited the acquisition of the spatial task, with a more gradual learning curve slope / longer escape latencies **(Fig. 3a)**. Although ISRIB only caused a small transient enhancement in sham surgery rats and $A\beta_{42\text{-}1}$-injected rats on day 2, ISRIB treatment consistently significantly shortened escape latencies in $A\beta_{1\text{-}42}$-injected rats from day 2 **(Fig. 3a)**. $A\beta_{1\text{-}42}$-injected rats crossed the platform area much less compared with sham surgery rats and $A\beta_{42\text{-}1}$ injected group when the platform was removed 24 h after the navigation training and ISRIB significantly reversed the memory deficit caused by $A\beta_{1\text{-}42}$ injection **(Fig. 3b)**. We also observed that $A\beta_{1\text{-}42}$-injected rats spent much less time in the target quadrant compared with sham surgery rats and $A\beta_{42\text{-}1}$ injected group in the probe trial and ISRIB treatment restored recall to normal level **(Fig. 3c)**. Both the total swim distance **(Fig. 3d)** and swim speed **(Fig. 3e)** were comparable in all the groups, which indicates that the movement ability was not affected.

ISRIB showed promising memory enhancing effects in wild type animals trained in the MWM with a weak protocos consisting of one swimming trial per day (11). Having not seen consistent memory enhancement in sham surgery or $A\beta_{42\text{-}1}$ injected animals trained in the MWM with a standard protocol, we performed navigation training with a weak protocol (1 trial per day) in rats 2 weeks after i.c.v. injection of $A\ß_{1\text{-}42}$ or reverse control $A\ß_{42\text{-}1}$ or age-matched rats with sham surgery. The same dose of ISRIB or vehicle were injected immediately after the training session every day. Although ISRIB significantly restored learning ability on days 6, 14 and 15 in animals that had been injected i.c.v with $A\ß_{1\text{-}42}$, this small molecule only caused a small transient enhancement in sham surgery rats and $A\beta_{42\text{-}1}$-injected rats on days 2-5 **(Fig. 4a)**. We also observed a memory deficit in $A\ß_{1\text{-}42}$ treated animals which crossed the platform area much less compared with $A\beta_{42\text{-}1}$-injected group or sham animals when the platform was removed 24 h after the navigation training and ISRIB significantly reversed the memory deficit cause by $A\ß_{1\text{-}42}$ injection **(Fig. 4b)**. Nevertheless, the target quadrant occupancy was comparably poor in all the groups during the probe trial **(Fig. 4c)**. Neither i.c.v injection of Aß peptide nor systemic injection of ISRIB affected the movement ability of rats because the swimming distance and speed were comparable in all the groups **(Fig. 4d, e)**. These results, together with our previous data, support the ability of ISRIB to abrogate learning and memory deficits caused by $A\ß_{1\text{-}42}$.

ISRIB restores ATF4 level without affecting aberrant phosphorylation of eIF2α in rat with exogenous Aβ injection

Elevated level of eIF2α phosphorylation have been observed in most studies of AD model animals with overexpression of Aβ (but see (28) (29)). eIF2α phosphorylation suppresses general protein synthesis and preferentially enhances translation of some mRNAs such as ATF4 which plays an important role in synaptic plasticity and memory. We then investigated the expression level of phosphorylated eIF2α and ATF4 in western blots of hippocampal tissue from rats that received an exogenous Aβ injection. The level of eIF2α phosphorylation was significantly increased in the hippocampus in $A\beta_{1\text{-}42}$ injected rats and treatment of ISRIB did not affect eIF2α phosphorylation caused by $A\beta_{1\text{-}42}$**(Fig. 5ab)**. Under $A\beta_{1\text{-}42}$ injection we observed a remarkable increase of ATF4 which ISRIB completely reversed **(Fig. 5cd)**.

Discussion

We report here that AD brain soluble Aβ causes loss of translational control in the promotion of LTD mechanisms in the dorsal hippocampus *in vivo*. Whereas normal LTD required de-novo protein synthesis, being completely prevented by the protein synthesis inhibitor emetine, we found that the same dose of emetine did not inhibit soluble Aβ-containing AD brain extract-facilitated hippocampal LTD. Remarkably, pre-treatment with ISRIB, at a dose that did not affect control LTD, completely prevented AD brain extract-facilitated LTD. Therefore, it seems likely that the restoration of normal protein synthesis by ISRIB prevents Aβ-facilitated LTD. This finding is consistent with prior evidence that certain forms of LTD, particular mGluR-dependent LTD, require eIF2α phosphorylation (30–33).

mGluR-LTD was prevented by either genetically reducing eIF2α phosphorylation or pharmacologically suppressing phospho-eIF2α controlled translation with ISRIB. By contrast, increased eIF2α phosphorylation by eIF2α phosphatases inhibitor Sal300 induces mGluR-LTD (30). Interestingly, mGluR-LTD is enhanced under pathophysiological conditions such as Fragile X syndrome (19) and AD Aβ (17). As shown here for AD Aβ-facilitated mGluR-LTD, Fragile X syndrome-faciltated mGluR-LTD is also resistant to protein synthesis inhibitors (19).

De novo protein synthesis-dependent synaptic plasticity is a likely critical step required for the generation of long-term memories. Consistent with an important role for the ISR in mediating a persistent disruption of synaptic learning mechanisms we found that ISRIB abrogated a learning and memory deficit caused by synthetic $A\beta_{1-42}$ in the water maze. Growing evidence indicates that eIF2α phosphorylation which is tightly regulated by four kinases (HRI, PKR, PERK and GCN2) is a memory suppressor. Either reduction of eIF2α phosphorylation or deletion / inhibition of the expression of any of the eIF2α kinases in the brain enhances memory in a variety of behavioral tasks (34–38). Conversely, increasing eIF2α phosphorylation, even when restricted to CA1 pyramidal neurons, impairs hippocampal memory consolidation (39). This study suggests that specific translational changes downstream of eIF2α phosphorylation are required for memory regulation.

Aberrant elevated phospho-eIF2α has been found in sporadic AD patients' brains (40–45) and in different transgenic mouse models of AD, including APP/PS1 (8) (46), Tg2576 (42, 47) and 5XFAD (43, 47, 48), (but see (28)). Post-mortem examination of the brains of the $A\beta_{1-42}$ injected rats showed that eIF2α phosphorylation and AFT4 were elevated by $A\beta_{1-42}$. ISRIB reduced AFT4 but not eIF2α phosphorylation. These findings are consistent with evidence that addition of oligomeric $A\beta_{1-42}$ induced aberrant expression of mRNAs of ATF4 (49, 50) and the putatitive mechanism of action of ISRIB. ISRIB reverses the attenuation of the guanine nucleotide exchange factor eIF2B by phosphorylated eIF2α (12, 13). ISRIB, unlike the PERK inhibitor GSK2606414, only partially restores protein synthesis and confers neuroprotection without adverse effects on the pancreas most probably due to its state-dependent action (14, 15, 51, 52).

ATF4 is a key regulator for hippocampal long-term synaptic plasticity and memory formation (32) and its expression level can be paradoxically upregulated by phosphorylation of eIF2α which leads to the inhibition of general protein synthesis. The protein level of ATF4 is increased in the cortex of AD brains (49, 53) and the increased translation level of ATF4 in axons is a mediator for the spread of AD pathology (49). ATF4 also binds to the regulatory region of human presenilin-1 gene and therefore is critical for gamma-secretase activity which in turn promotes the production of Aβ (54). Our administration of ISRIB restores the elevated level of ATF4 caused by Aβ. These results are consistent with reports that ISRIB blocks the production of ATF4 upon GCN2 or HRI activation (11, 55). However, whether restoration of ATF4 mediated the protective effects of ISRIB in our Aβ-injected rat model is not clear and further investigation is needed.

Apart from ER stress caused by the unfolded protein response, other Aβ-mediated AD pathologies including glutamate excitotoxicity, hypoxia and neuronal inflammation can also induce the ISR. Both Aβ-containing AD brain extracts and purified Aβ dimers potentially suppress glutamate reuptake and subsequently induce neuronal hyperactivation (56). Hypoxia with decreased cerebral blood flow has been found early in AD and a body of evidence indicates that Aβ has vasoactive and vasculotoxic effects on blood vessels, in particular capillaries at pericyte locations (57).

Some reports indicate that ISRIB is not effective in certain transgenic APP and tau mouse models, possibly because of ISRIB's pharmacological profile or differences in the level of engagement of the ISR in these models (28, 29, 58–60) and some recent studies indicate that ER stress is not elevated in certain transgenic mouse models of AD (28, 29, 60). The very high failure rate of AD clinical trials may be partly due to the premature translation of successful pathology reduction in transgenic mice to humans (61). Thus, choosing appropriate models in AD research is extremely important and the best strategy is to perform studies using human tissues whenever possible before developing ideal animal models (62). Compared with transgenic models, whether or not animal models incorporating injected soluble Aβ from AD brain here more closely mimic key early pathological changes in AD patient needs to be carefully addressed in future studies.

Conclusions

In summary, exogenous Aβ triggers the ISR in the hippocampus with aberrant high level of phosphorylated eIF2α and ATF4. The small molecule ISRIB provides promising protective effects on our Aβ-facilitated LTD model and Aβ-induced spatial learning and memory deficit. Targeting the ISR by suppressing the eIF2α cascade with ISRIB may provide protective effects against the synaptic and cognitive disruptive effects of Aβ which likely mediate the early stage of sporadic AD.

Abbreviations

AD
Alzheimer's disease
ATF4
the activating transcription factor 4
Aβ
amyloid-β-protein
eIF2α
the eukaryotic initiation factor 2 α-subunit
eIF2B
the eukaryotic initiation factor 2B
GCN2
the general control nonderepressible 2
HRI

the heme-regulated inhibitor kinase
ISR
the integrated stress response
LFS
low frequency stimulation
LTD
long-term depression
LTP
long-term potentiation
mGluR
the metabotropic glutamate receptor
MWM
the Morris water maze
PERK
the protein kinase R-like endoplasmic reticulum kinase
PKR
the double-stranded RNA-activated protein kinase
UPR
the unfolded protein response

Declarations

Availability of data and materials

All data supporting this study are available from the corresponding author upon reasonable request.

Acknowledgements

We would like to thank Dr. D. M. Walsh from Brigham and Women's Hospital and Harvard Medical School (Boston, MA) for providing TBS extracts of human brain and Dr. D. Duan from Zhengzhou University School of Medicine (China) for advising us on Morris water maze.

Funding

Research reported here was supported by National Natural Science Foundation of China (No. 81471114 to NWH, No. 81670301 to DW), Zhengzhou University (140/32310295 to NWH) and by Science Foundation Ireland (10/IN.1/B3001 and 14/IA/2571 to MJR).

Contributions

NWH and MJR conceived the idea, directed experiments and wrote the manuscript; ZH, PY, DW, YW, YY and JX performed Morris water maze, Western Blot ; NWH, YQ, TO and IK conducted the electrophysiological experiments. All authors contributed to preparing figures and writing the manuscript.

Corresponding author

Correspondence to Michael J Rowan or Neng-Wei Hu

Ethics declarations

Ethics approval and consent to participate

As reported previously (17), the AD brain was obtained and used in accordance with the UCD Human Research Ethics Committee guidelines (under approval LS-E-10-10-Walsh) and TCD Faculty of Health Science Ethics Committee (under approval 16014). Informed consent was obtained from subject. Samples of temporal cortex were obtained from the brain which was from an 85-year-old male with dementia and fulminant amyloid and tangle pathology (Braak stage = 4) and was provided by Drs Dykoski and Cleary of Minneapolis VA Health Care System.

Animal care and experimental protocols followed the ARRIVE (Animal Research: Reporting of In Vivo Experiments) guidelines 2.0 (16) and were approved by the Health Products Regulatory Authority, Ireland and Animal Care and Use Committee of Zhengzhou University and Wannan Medical College, China.

Consent for publication

N/A

Competing interests

The authors declare no competing financial interests.

References

1. Costa-Mattioli M, Walter P. The integrated stress response: From mechanism to disease. Science. 2020;368(6489).
2. Pakos-Zebrucka K, Koryga I, Mnich K, Ljujic M, Samali A, Gorman AM. The integrated stress response. EMBO Rep. 2016;17(10):1374-95.
3. B'Chir W, Maurin AC, Carraro V, Averous J, Jousse C, Muranishi Y, et al. The eIF2alpha/ATF4 pathway is essential for stress-induced autophagy gene expression. Nucleic Acids Res. 2013;41(16):7683-99.
4. Yang SY, Wei FL, Hu LH, Wang CL. PERK-eIF2alpha-ATF4 pathway mediated by endoplasmic reticulum stress response is involved in osteodifferentiation of human periodontal ligament cells under cyclic mechanical force. Cell Signal. 2016;28(8):880-6.
5. Roussel BD, Kruppa AJ, Miranda E, Crowther DC, Lomas DA, Marciniak SJ. Endoplasmic reticulum dysfunction in neurological disease. Lancet Neurol. 2013;12(1):105-18.

6. Stutzbach LD, Xie SX, Naj AC, Albin R, Gilman S, Group PSPGS, et al. The unfolded protein response is activated in disease-affected brain regions in progressive supranuclear palsy and Alzheimer's disease. Acta Neuropathol Commun. 2013;1:31.
7. Moon SL, Sonenberg N, Parker R. Neuronal Regulation of eIF2alpha Function in Health and Neurological Disorders. Trends Mol Med. 2018;24(6):575-89.
8. Ma T, Trinh MA, Wexler AJ, Bourbon C, Gatti E, Pierre P, et al. Suppression of eIF2alpha kinases alleviates Alzheimer's disease-related plasticity and memory deficits. Nat Neurosci. 2013;16(9):1299-305.
9. Hetz C, Saxena S. ER stress and the unfolded protein response in neurodegeneration. Nat Rev Neurol. 2017;13(8):477-91.
10. Gonzalez-Teuber V, Albert-Gasco H, Auyeung VC, Papa FR, Mallucci GR, Hetz C. Small Molecules to Improve ER Proteostasis in Disease. Trends Pharmacol Sci. 2019;40(9):684-95.
11. Sidrauski C, Acosta-Alvear D, Khoutorsky A, Vedantham P, Hearn BR, Li H, et al. Pharmacological brake-release of mRNA translation enhances cognitive memory. Elife. 2013;2:e00498.
12. Tsai JC, Miller-Vedam LE, Anand AA, Jaishankar P, Nguyen HC, Renslo AR, et al. Structure of the nucleotide exchange factor eIF2B reveals mechanism of memory-enhancing molecule. Science. 2018;359(6383).
13. Zyryanova AF, Weis F, Faille A, Alard AA, Crespillo-Casado A, Sekine Y, et al. Binding of ISRIB reveals a regulatory site in the nucleotide exchange factor eIF2B. Science. 2018;359(6383):1533-6.
14. Halliday M, Radford H, Sekine Y, Moreno J, Verity N, le Quesne J, et al. Partial restoration of protein synthesis rates by the small molecule ISRIB prevents neurodegeneration without pancreatic toxicity. Cell Death Dis. 2015;6:e1672.
15. Rabouw HH, Langereis MA, Anand AA, Visser LJ, de Groot RJ, Walter P, et al. Small molecule ISRIB suppresses the integrated stress response within a defined window of activation. Proc Natl Acad Sci U S A. 2019;116(6):2097-102.
16. Percie du Sert N, Hurst V, Ahluwalia A, Alam S, Avey MT, Baker M, et al. The ARRIVE guidelines 2.0: Updated guidelines for reporting animal research. PLoS Biol. 2020;18(7):e3000410.
17. Hu NW, Nicoll AJ, Zhang D, Mably AJ, O'Malley T, Purro SA, et al. mGlu5 receptors and cellular prion protein mediate amyloid-beta-facilitated synaptic long-term depression in vivo. Nat Commun. 2014;5:3374.
18. Sossin WS, Costa-Mattioli M. Translational Control in the Brain in Health and Disease. Cold Spring Harb Perspect Biol. 2019;11(8).
19. Nosyreva ED, Huber KM. Metabotropic receptor-dependent long-term depression persists in the absence of protein synthesis in the mouse model of fragile X syndrome. J Neurophysiol. 2006;95(5):3291-5.
20. Nicholls RE, Alarcon JM, Malleret G, Carroll RC, Grody M, Vronskaya S, et al. Transgenic mice lacking NMDAR-dependent LTD exhibit deficits in behavioral flexibility. Neuron. 2008;58(1):104-17.

21. Dong Z, Bai Y, Wu X, Li H, Gong B, Howland JG, et al. Hippocampal long-term depression mediates spatial reversal learning in the Morris water maze. Neuropharmacology. 2013;64:65-73.
22. Connor SA, Wang YT. A Place at the Table: LTD as a Mediator of Memory Genesis. Neuroscientist. 2016;22(4):359-71.
23. Benarroch EE. Glutamatergic synaptic plasticity and dysfunction in Alzheimer disease: Emerging mechanisms. Neurology. 2018;91(3):125-32.
24. Li S, Selkoe DJ. A mechanistic hypothesis for the impairment of synaptic plasticity by soluble Abeta oligomers from Alzheimer's brain. J Neurochem. 2020.
25. Nakamura S, Murayama N, Noshita T, Annoura H, Ohno T. Progressive brain dysfunction following intracerebroventricular infusion of beta(1-42)-amyloid peptide. Brain Res. 2001;912(2):128-36.
26. Kim HY, Lee DK, Chung BR, Kim HV, Kim Y. Intracerebroventricular Injection of Amyloid-beta Peptides in Normal Mice to Acutely Induce Alzheimer-like Cognitive Deficits. J Vis Exp. 2016(109).
27. Ikram M, Muhammad T, Rehman SU, Khan A, Jo MG, Ali T, et al. Hesperetin Confers Neuroprotection by Regulating Nrf2/TLR4/NF-kappaB Signaling in an Abeta Mouse Model. Mol Neurobiol. 2019;56(9):6293-309.
28. Sadleir KR, Popovic J, Vassar R. ER stress is not elevated in the 5XFAD mouse model of Alzheimer's disease. J Biol Chem. 2018;293(48):18434-43.
29. Hashimoto S, Ishii A, Kamano N, Watamura N, Saito T, Ohshima T, et al. Endoplasmic reticulum stress responses in mouse models of Alzheimer's disease: Overexpression paradigm versus knockin paradigm. J Biol Chem. 2018;293(9):3118-25.
30. Di Prisco GV, Huang W, Buffington SA, Hsu CC, Bonnen PE, Placzek AN, et al. Translational control of mGluR-dependent long-term depression and object-place learning by eIF2alpha. Nat Neurosci. 2014;17(8):1073-82.
31. Trinh MA, Ma T, Kaphzan H, Bhattacharya A, Antion MD, Cavener DR, et al. The eIF2alpha kinase PERK limits the expression of hippocampal metabotropic glutamate receptor-dependent long-term depression. Learn Mem. 2014;21(5):298-304.
32. Pasini S, Corona C, Liu J, Greene LA, Shelanski ML. Specific downregulation of hippocampal ATF4 reveals a necessary role in synaptic plasticity and memory. Cell Rep. 2015;11(2):183-91.
33. Huang W, Placzek AN, Viana Di Prisco G, Khatiwada S, Sidrauski C, Krnjevic K, et al. Translational control by eIF2alpha phosphorylation regulates vulnerability to the synaptic and behavioral effects of cocaine. Elife. 2016;5.
34. Costa-Mattioli M, Gobert D, Harding H, Herdy B, Azzi M, Bruno M, et al. Translational control of hippocampal synaptic plasticity and memory by the eIF2alpha kinase GCN2. Nature. 2005;436(7054):1166-73.
35. Costa-Mattioli M, Gobert D, Stern E, Gamache K, Colina R, Cuello C, et al. eIF2alpha phosphorylation bidirectionally regulates the switch from short- to long-term synaptic plasticity and memory. Cell. 2007;129(1):195-206.

36. Zhu PJ, Huang W, Kalikulov D, Yoo JW, Placzek AN, Stoica L, et al. Suppression of PKR promotes network excitability and enhanced cognition by interferon-gamma-mediated disinhibition. Cell. 2011;147(6):1384-96.
37. Stern E, Chinnakkaruppan A, David O, Sonenberg N, Rosenblum K. Blocking the eIF2alpha kinase (PKR) enhances positive and negative forms of cortex-dependent taste memory. J Neurosci. 2013;33(6):2517-25.
38. Ounallah-Saad H, Sharma V, Edry E, Rosenblum K. Genetic or pharmacological reduction of PERK enhances cortical-dependent taste learning. J Neurosci. 2014;34(44):14624-32.
39. Jiang Z, Belforte JE, Lu Y, Yabe Y, Pickel J, Smith CB, et al. eIF2alpha Phosphorylation-dependent translation in CA1 pyramidal cells impairs hippocampal memory consolidation without affecting general translation. J Neurosci. 2010;30(7):2582-94.
40. Chang RC, Wong AK, Ng HK, Hugon J. Phosphorylation of eukaryotic initiation factor-2alpha (eIF2alpha) is associated with neuronal degeneration in Alzheimer's disease. Neuroreport. 2002;13(18):2429-32.
41. Hoozemans JJ, Veerhuis R, Van Haastert ES, Rozemuller JM, Baas F, Eikelenboom P, et al. The unfolded protein response is activated in Alzheimer's disease. Acta Neuropathol. 2005;110(2):165-72.
42. Kim HS, Choi Y, Shin KY, Joo Y, Lee YK, Jung SY, et al. Swedish amyloid precursor protein mutation increases phosphorylation of eIF2alpha in vitro and in vivo. J Neurosci Res. 2007;85(7):1528-37.
43. O'Connor T, Sadleir KR, Maus E, Velliquette RA, Zhao J, Cole SL, et al. Phosphorylation of the translation initiation factor eIF2alpha increases BACE1 levels and promotes amyloidogenesis. Neuron. 2008;60(6):988-1009.
44. Mouton-Liger F, Paquet C, Dumurgier J, Bouras C, Pradier L, Gray F, et al. Oxidative stress increases BACE1 protein levels through activation of the PKR-eIF2alpha pathway. Biochim Biophys Acta. 2012;1822(6):885-96.
45. Natunen T, Parrado AR, Helisalmi S, Pursiheimo JP, Sarajarvi T, Makinen P, et al. Elucidation of the BACE1 regulating factor GGA3 in Alzheimer's disease. J Alzheimers Dis. 2013;37(1):217-32.
46. Hong J, Hong SG, Lee J, Park JY, Eriksen JL, Rooney BV, et al. Exercise training ameliorates cerebrovascular dysfunction in a murine model of Alzheimer's disease: role of the P2Y2 receptor and endoplasmic reticulum stress. Am J Physiol Heart Circ Physiol. 2020;318(6):H1559-H69.
47. Borreca A, Valeri F, De Luca M, Ernst L, Russo A, Nobili A, et al. Transient upregulation of translational efficiency in prodromal and early symptomatic Tg2576 mice contributes to Abeta pathology. Neurobiol Dis. 2020;139:104787.
48. Hwang KD, Bak MS, Kim SJ, Rhee S, Lee YS. Restoring synaptic plasticity and memory in mouse models of Alzheimer's disease by PKR inhibition. Mol Brain. 2017;10(1):57.
49. Baleriola J, Walker CA, Jean YY, Crary JF, Troy CM, Nagy PL, et al. Axonally synthesized ATF4 transmits a neurodegenerative signal across brain regions. Cell. 2014;158(5):1159-72.
50. Nakagawa T, Ohta K. Quercetin Regulates the Integrated Stress Response to Improve Memory. Int J Mol Sci. 2019;20(11).

51. Chou A, Krukowski K, Jopson T, Zhu PJ, Costa-Mattioli M, Walter P, et al. Inhibition of the integrated stress response reverses cognitive deficits after traumatic brain injury. Proc Natl Acad Sci U S A. 2017;114(31):E6420-E6.
52. Zhu PJ, Khatiwada S, Cui Y, Reineke LC, Dooling SW, Kim JJ, et al. Activation of the ISR mediates the behavioral and neurophysiological abnormalities in Down syndrome. Science. 2019;366(6467):843-9.
53. Lewerenz J, Maher P. Basal levels of eIF2alpha phosphorylation determine cellular antioxidant status by regulating ATF4 and xCT expression. J Biol Chem. 2009;284(2):1106-15.
54. Mitsuda T, Hayakawa Y, Itoh M, Ohta K, Nakagawa T. ATF4 regulates gamma-secretase activity during amino acid imbalance. Biochem Biophys Res Commun. 2007;352(3):722-7.
55. Hosoi T, Kakimoto M, Tanaka K, Nomura J, Ozawa K. Unique pharmacological property of ISRIB in inhibition of Abeta-induced neuronal cell death. J Pharmacol Sci. 2016;131(4):292-5.
56. Zott B, Simon MM, Hong W, Unger F, Chen-Engerer HJ, Frosch MP, et al. A vicious cycle of beta amyloid-dependent neuronal hyperactivation. Science. 2019;365(6453):559-65.
57. Nortley R, Korte N, Izquierdo P, Hirunpattarasilp C, Mishra A, Jaunmuktane Z, et al. Amyloid beta oligomers constrict human capillaries in Alzheimer's disease via signaling to pericytes. Science. 2019;365(6450).
58. Johnson EC, Kang J. A small molecule targeting protein translation does not rescue spatial learning and memory deficits in the hAPP-J20 mouse model of Alzheimer's disease. PeerJ. 2016;4:e2565.
59. Briggs DI, Defensor E, Memar Ardestani P, Yi B, Halpain M, Seabrook G, et al. Role of Endoplasmic Reticulum Stress in Learning and Memory Impairment and Alzheimer's Disease-Like Neuropathology in the PS19 and APP(Swe) Mouse Models of Tauopathy and Amyloidosis. eNeuro. 2017;4(4).
60. Pitera AP, Asuni AA, O'Connor V, Deinhardt K. Pathogenic tau does not drive activation of the unfolded protein response. J Biol Chem. 2019;294(25):9679-88.
61. Cummings J. Lessons Learned from Alzheimer Disease: Clinical Trials with Negative Outcomes. Clin Transl Sci. 2018;11(2):147-52.
62. Drummond E, Wisniewski T. Alzheimer's disease: experimental models and reality. Acta Neuropathol. 2017;133(2):155-75.

Figures

Fig 1

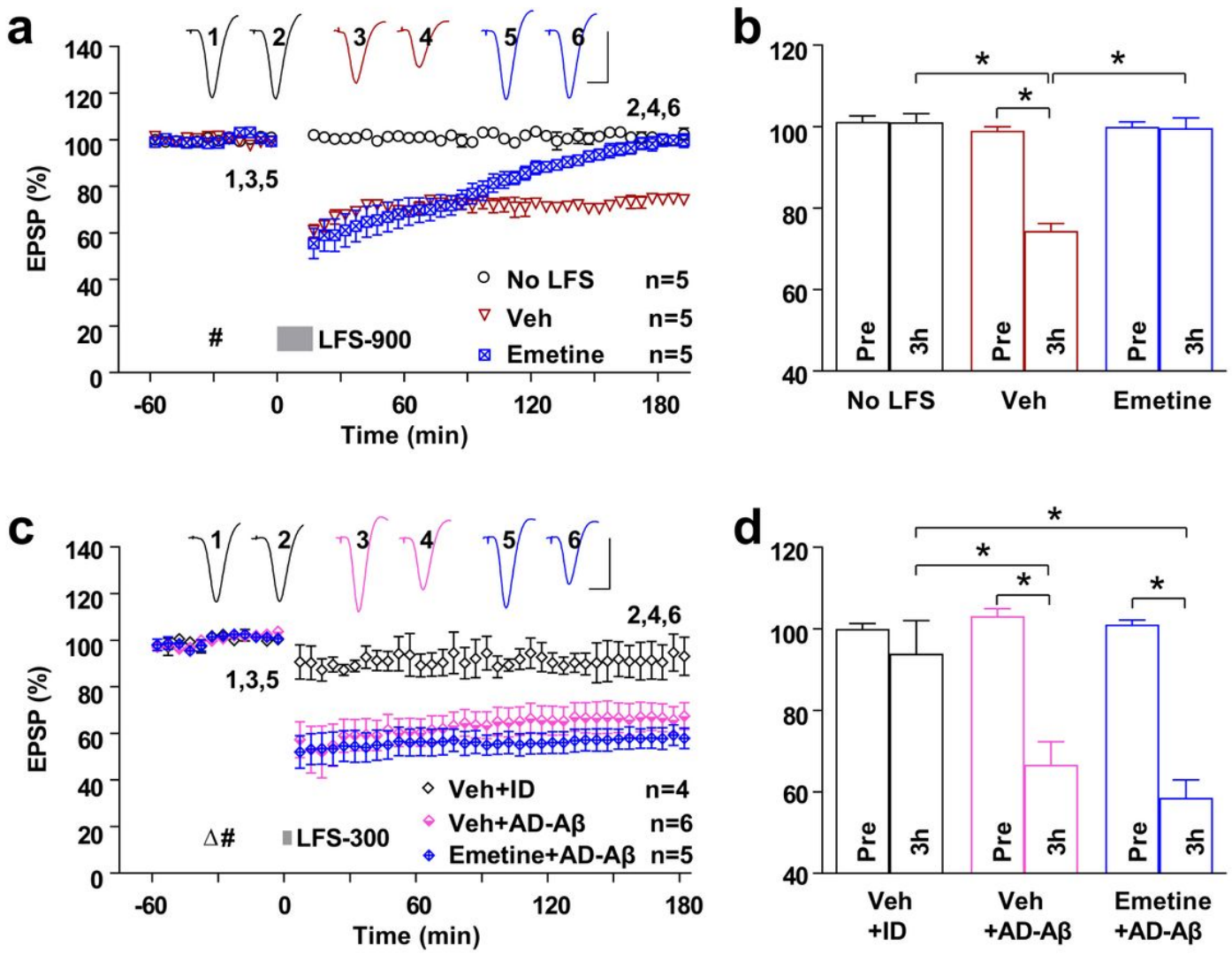

Figure 1

The maintenance of Aß-facilitated LTD, unlike control LTD, is not blocked by the protein synthesis inhibitor emetine. (a) Whereas LFS-900 (bar, 900 high-intensity pulses at 1 Hz) 30min after acute intracerebroventricular (i.c.v.) injection of vehicle trigged a robust and persistent LTD, the later phase of control LTD was completely blocked in animals treated with emetine (240 µg, i.c.v.). As summarized in (b) at 3 h after LFS-900 the EPSP measured 99.6 ± 2.5% in the emetine treated group, n = 5, P = 0.8972 compared with baseline (Pre), paired t; P < 0.0001 compared with 74.4 ± 1.8% in the vehicle control group, one-way ANOVA). (c) Soluble AD brain Aß facilitates LTD that is resistant to emetine. The application of weak LFS (bar, LFS-300; 300 high-intensity pulses at 1 Hz) trigged a robust and persistent LTD 30 min after i.c.v. injection of unmanipulated TBS extract of AD brain (AD-Aß, 5 µl). In contrast, in animals treated with the same extract of AD brain that had been immunodepleted of Aß using a polyclonal anti-Aß

antibody (ID), LFS-300 failed to induce LTD. Fifteen minutes before i.c.v. injection of AD-Aß, i.c.v. administration of emetine (240 µg) did not significantly affect AD-facilitated LTD. Triangle: Vehicle or Emetine; hash: AD-Aß or ID. As summarized in (d) at 3 h the EPSP measured 93.9 ± 8.1% in Veh+ID group (n = 4, P = 0.4459 compared with Pre; paired t), 66.7 ± 5.7% in Veh+ AD-Aß group (n = 6, P = 0.0013 compared with Pre and P = 0.0247 compared with Veh+ID group; paired t and one-way ANOVA) and 58.6 ± 4.4% in Emetine+ AD-Aß (n = 5, P = 0.0015 compared with Pre and P > 0.9999 compared with Veh+ AD-Aß group; paired t and one-way ANOVA). Calibration bars for EPSP traces: vertical, 2 mV; horizontal, 10 ms.

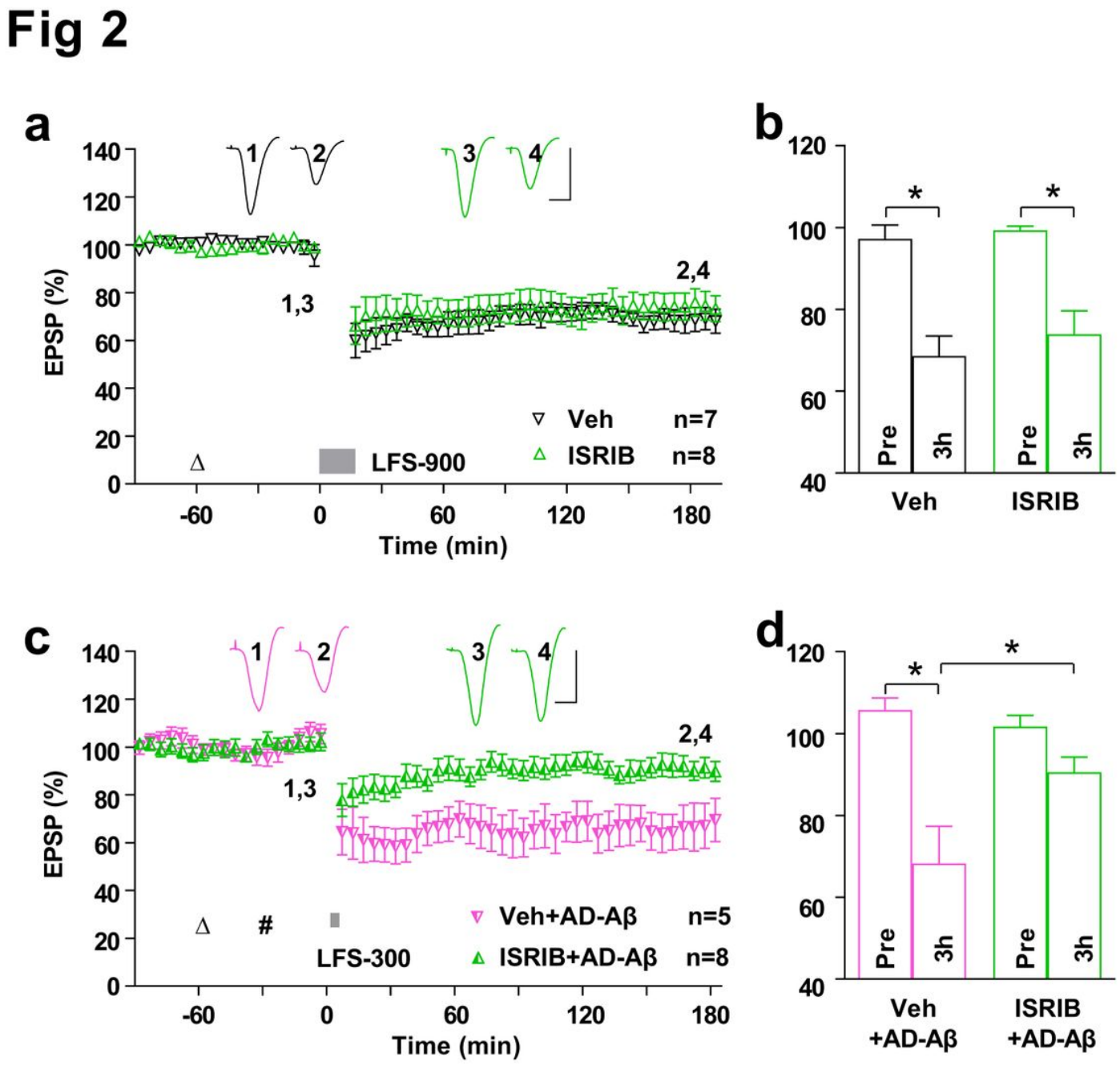

Figure 2

Aß-facilitated LTD, but not control LTD, is blocked by the integrated stress inhibitor ISRIB. (a) In both vehicle (1:1 DMSO and PEG400, i.p.) and ISRIB (2.5mg/kg, i.p.) pre-treated rats, the application of LFS-900 trigged a robust and persistent LTD. As summarized in (b) at 3 h the EPSP measured 73.9 ± 5.7% in ISRIB treated group, n = 8, P = 0.4970 compared with 68.6 ± 4.9% in the vehicle control group; unpaired t). (c) In contrast, the same dose of ISRIB that did not affect control LTD induced by LFS-900 completely blocked the maintenance of Aβ-facilitated LTD. Thus, whereas weak LFS (bar, LFS-300) trigged a robust and persistent LTD after administration of soluble Aß-containing AD brain extract (AD-Aß, 5 µl, i.c.v.) in vehicle pre-injected rats, LTD was strongly inhibited in ISRIB treated rats. (d) Summary at 3 h (90.6 ± 3.7% in the ISRIB treated group, n = 5, P = 0.0786 compared with Pre, P = 0.0231 compared with 68.3 ± 9.1% in the AD-Aβ group; paired t and unpaired t). Triangle: Vehicle or ISRIB; hash: AD-Aß. Calibration bars for EPSP traces: vertical, 2 mV; horizontal, 10 ms.

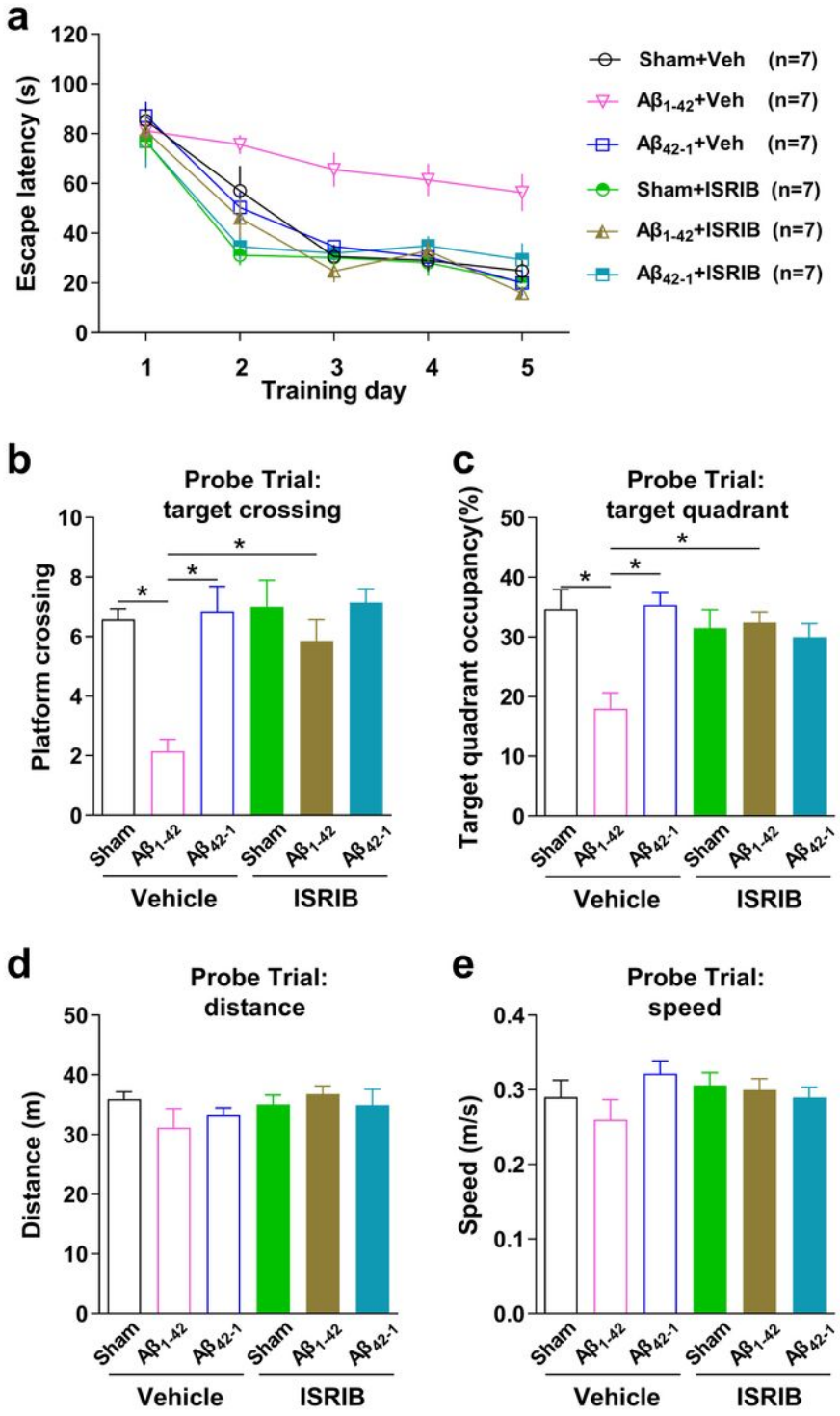

Figure 3

Facilitation of learning and memory by ISRIB in Aß1-42-injected rats using a standard MWM protocol. (a) Water maze training (4 trials per day for 5 days) was performed 2 weeks after i.c.v. injection of Aß1-42 or reverse control Aß42-1. Vehicle (1% DMSO in saline) or ISRIB (0.25mg/kg, i.p.) were injected immediately after the last training trial in the MWM every day. Escape latency in the navigation trial plotted against the training days. Two-way ANOVA followed by a post hoc Bonferroni multiple comparison test, $P < 0.0001$,

F5,36 = 15.38. During training, compared with the Aß42-1+Veh and Sham+Veh group, the Aß1-42+Veh group spent more time to escape to the hidden platform from day 3 (Aß1-42+Veh versus Sham+Veh: P = 0.0079 on day 3, P = 0.0101 on day 4, P = 0.0229 on day 5; Aß1-42+Veh versus Aß42-1+Veh: P = 0.0165 on day 3, P = 0.0118 on day 4, P = 0.0107 on day 5) but not in the first 2 days. However, a large reduction in escape latency was caused by ISRIB in rats injected with Aß1-42 from day 2 (Aß1-42+Veh versus Aß1-42+ISRIB: P = 0.0362). (b) In the probe trial, Aß1-42+Veh animals appeared to cross the platform less frequently compared with the Aß42-1+Veh and Sham+Veh group and ISRIB significantly improved performance (P = 0.0001, one-way ANOVA followed by a post hoc Bonferroni multiple comparison test). (c) In the case of the probe trial quadrant bias, ISRIB significantly enhanced target quadrant occupancy in the Aß1-42 -injected animals (Aß1-42+Veh versus Aß1-42+ISRIB: P < 0.0020, one-way ANOVA followed by a post hoc Bonferroni multiple comparison test). (d,e) Both total swimming distance (P = 0.4351, one-way ANOVA) and swimming speed (P = 0.3626, one-way ANOVA) are comparable in all the groups. Error bars, s.e.m.

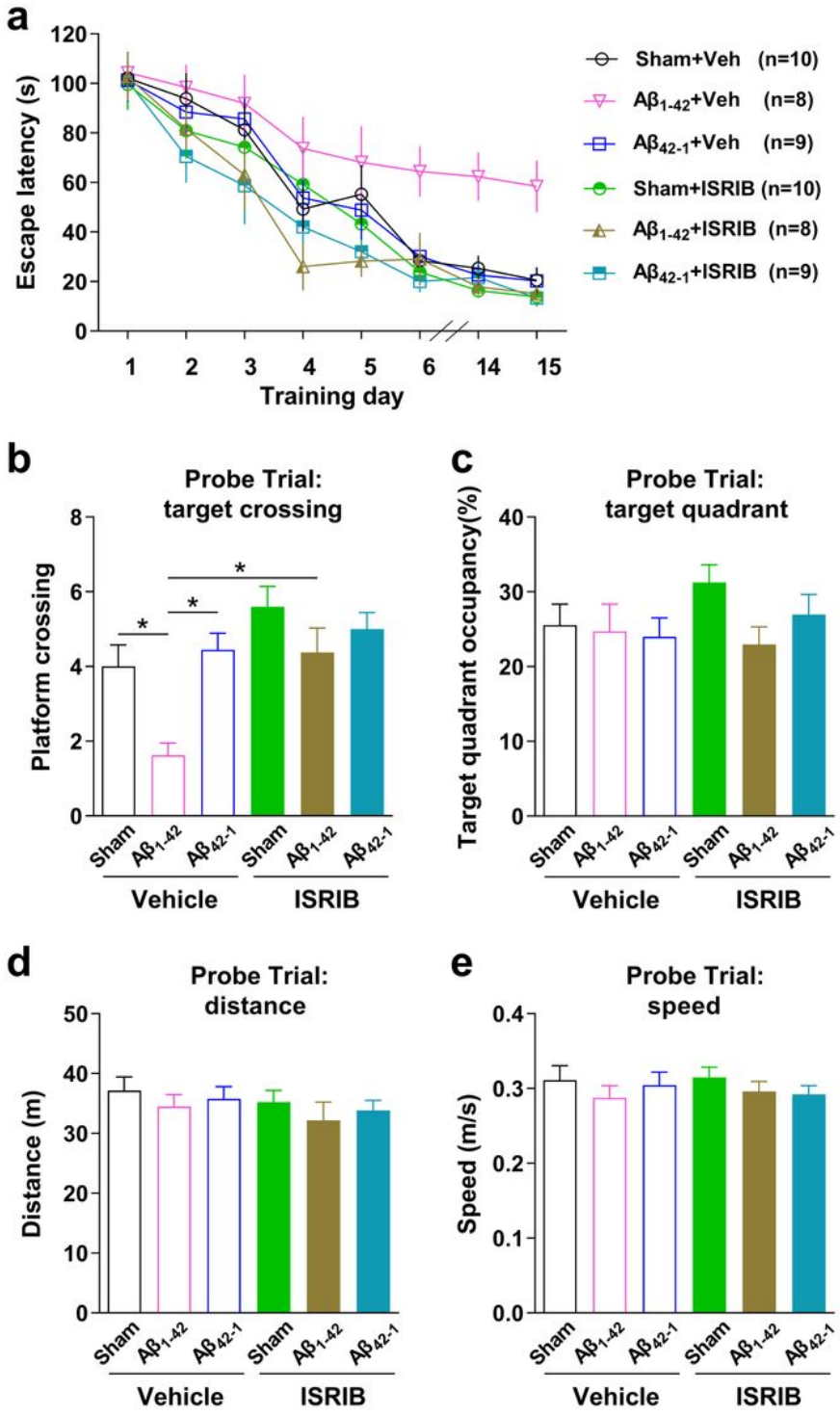

Figure 4

Spatial learning and memory deficits in Aß1-42-injected rats are abrogated by ISRIB using a weak MWM training protocol. (a) All animals were trained with 1-trial / day. Because the day-to-day decrease in escape latency over the first six days was very slow compared with the results from daily 4-trial training. training was resumed for two days after a 7-day break. Vehicle or ISRIB (0.25mg/kg, i.p.) were injected immediately after the training session in the MWM every day. All the rats spent less time gradually to find

the hidden platform after each training trial. Aß1-42-injected rats spent more time to find the hidden platform from day 6 and on day 14 and day 15 after one-week break (Two-way ANOVA followed by a post hoc Bonferroni multiple comparison test, $P < 0.0001$, $F_{5,48} = 8.778$. Aß1-42+Veh versus Sham+Veh: $P = 0.0681$ on day 6, $P = 0.0325$ on day 14, $P = 0.0415$ on day 15; Aß1-42+Veh versus Aß42-1+Veh: $P = 0.1142$ on day 6, $P = 0.0207$ on day 14, $P = 0.0410$ on day 15) and ISRIB significantly improved performance (Aß1-42+Veh versus Aß1-42+ISRIB: $P = 0.0146$ on day 6, $P = 0.0231$ on day 14, $P = 0.0158$ on day 15). No difference was detected among Sham+Veh, Aß42-1+Veh, Sham+ISRIB, Aß42-1+ISRIB and Aß1-42+ISRIB groups (Repeated measures ANOVA. $P = 0.0569$, $F_{4,41} = 2.504$). (b) In the probe trial, Aß1-42-injected animals crossed the platform much less compared with control groups (Aß1-42+Veh versus Sham+Veh: $P = 0.0129$; Aß1-42+Veh versus Aß42-1+Veh: $P = 0.0028$) and ISRIB significantly enhanced platform crossing in Aß1-42-injected rats (Aß1-42+Veh versus Aß1-42+ISRIB: $P = 0.0050$, One-way ANOVA followed by a post hoc Bonferroni multiple comparison test). (c-e) All the groups were similar in target quadrant occupancy ($P = 0.9409$, One-way ANOVA) (c) and total swimming distance ($P = 0.7056$, One-way ANOVA) (d) and swimming speed ($P = 0.7876$, One-way ANOVA) (e). Error bars, s.e.m.

Fig 5

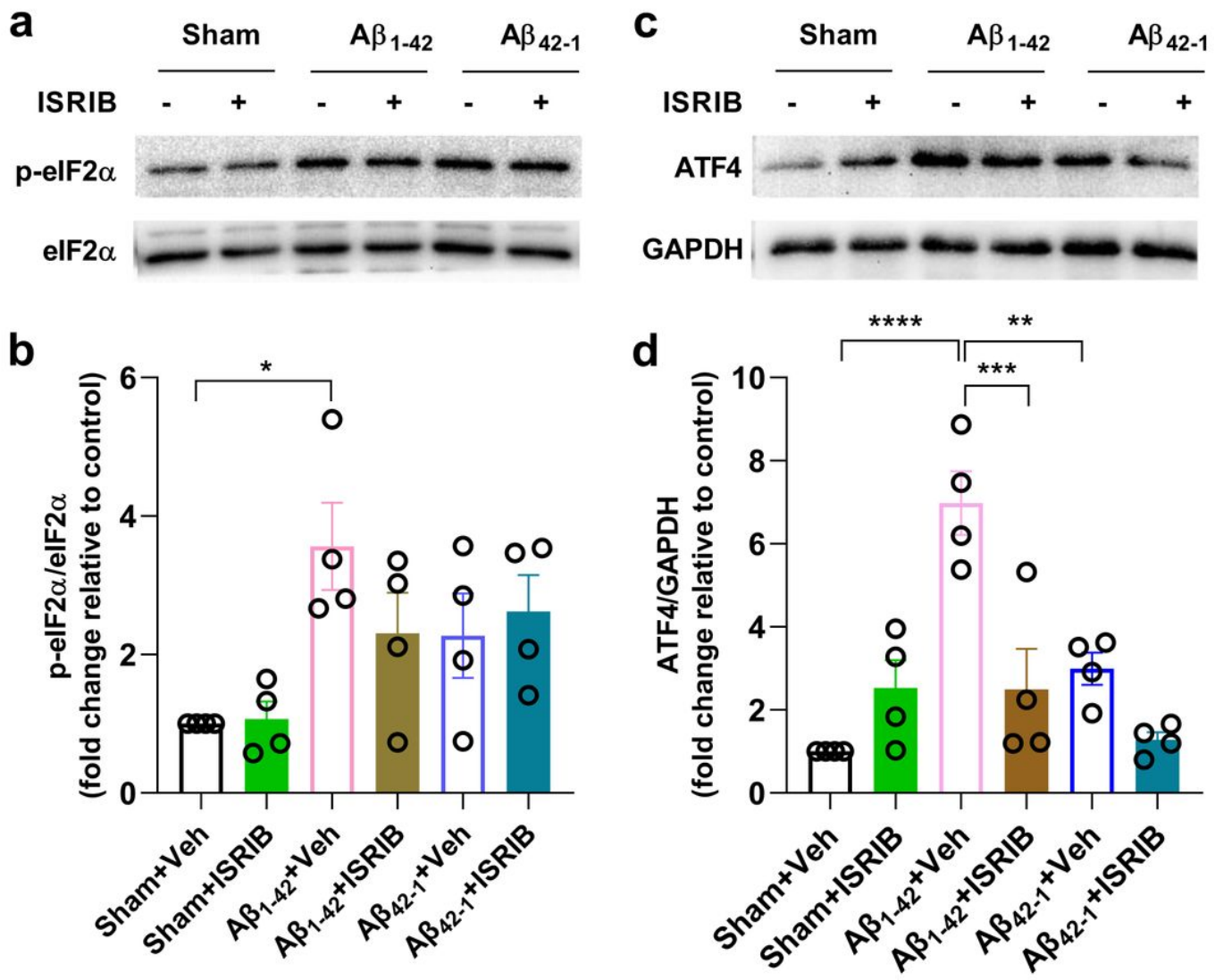

Figure 5

ATF4 but not eIF2α phosphorylation, is restored by ISRIB in Aß1-42-injected rats. (a,b) Western blots showing that the level of phospho-eIF2α was increased in the hippocampus of rats about three weeks (two weeks recovery plus one week MWM test) after i.c.v. injection of Aß1-42 (n = 4, P = 0.0102, Aß1-42+Veh compared with Sham+Veh group; one-way ANOVA) while the injection of the reverse sequence peptide Aß42-1 did not obviously change the level of phospho-eIF2α (n = 4, P = 0.5057, Aß42-1+Veh compared with Sham+Veh group; one-way ANOVA). Treatment of ISRIB (0.25mg/kg, i.p.) for 5 days did not affect the levels of phospho-eIF2α in Aß1-42-injected rats (n = 4, P = 0.5240, Aß1-42+Veh compared with Aß1-42+ISRIB group; one-way ANOVA). (c,d) The level of ATF4 increased in Aß1-42 -injected rats (n = 4, P < 0.0001, Aß1-42+Veh compared with Sham+Veh or Aß42-1+Veh group; one-way ANOVA) but the injection of the reverse sequence peptide Aß42-1 did not change the level of ATF4 (n = 4, P = 0.2133,

Aß42-1+Veh compared with Sham+Veh group; one-way ANOVA). Treatment of ISRIB restored ATF4 to normal level (n = 4, P = 0.0004, Aß1-42+Veh compared with Aß1-42+ISRIB; P = 0.6636, Aß1-42+ISRIB compared with Sham+Veh group; one-way ANOVA). Error bars, s.e.m.